


 Cite this: *RSC Adv.*, 2020, 10, 19615

## Continuous production and properties of multi-level nanofiber air filters by blow spinning†

 Jianan Song,<sup>‡a</sup> Zhenglian Liu,<sup>‡b</sup> Ziwei Li<sup>a</sup> and Hui Wu<sup>ID\* a</sup>

Nanofibers are gradually being widely used in air filtration due to their unique characteristics. However, the mass production of nanofiber filter material faces several problems. Blow spinning is an emerging technology, which have great potential for mass production of nanofibers. In this work, we have successfully realized the continuous production of 500 mm wide nanofiber membranes by blow spinning, which enables continuous preparation of multi-level nanofiber filter materials: PAN60 (filtration efficiency is 63.2%, pressure drop is 18 Pa), PAN80 (filtration efficiency is 80.7%, pressure drop is 38 Pa), PAN90 (filtration efficiency is 92.9%, pressure drop is 58 Pa) and PAN99 (filtration efficiency is 99.5%, pressure drop is 123 Pa). In order to improve the stability performance of melt-blown filters, we provide a strategy that combines nanofibers with a melt-blown filter. PAN nanofibers were sprayed directly on the melt-blown filter by blow spinning. The composite filters have more stable filtration performance and higher efficiency when intercepting particles with a diameter below 100 nm than melt-blown filters.

 Received 21st February 2020  
 Accepted 22nd April 2020

DOI: 10.1039/d0ra01656j

[rsc.li/rsc-advances](http://rsc.li/rsc-advances)

Air pollution has become the biggest ecological environment problem, seriously affecting human health and life.<sup>1–3</sup> One of the most serious forms of air pollution is particulate matter pollution. Air particulate matter pollution (PM) is a complex mixture, which contains fine particulate matter and small droplets. It generally comes from industrial and automotive exhaust emissions and secondary generation of nitrogen oxides in the atmosphere.<sup>4,5</sup> In terms of particle size, PM is mainly divided into PM10 and PM2.5. PM10 means that the air equivalent particle size is less than 10 μm, and PM2.5 means that the air equivalent particle size is less than 2.5 μm. PM2.5 carries a large number of toxic compounds and poses a huge threat to human health due to its small size, which can penetrate human lungs and bronchi. Many studies demonstrate that prolonged exposure to high concentrations of PM2.5 will increase the incidence of many diseases such as lung cancer, cardiovascular disease, asthma and so on.<sup>6,7</sup> Nowadays, the use of fossil energy in developing countries, such as coal, has caused a lot of PM2.5 pollution. It will exist in the atmosphere for several weeks, so many areas are facing long-term severe haze weather. In haze weather, high concentration of PM2.5 affects air quality and people's travel, causing great psychological and physiological trauma.<sup>8</sup>

In order to reduce the harm of PM2.5 to people, masks, air purifiers and fresh air systems have been widely used. Filter materials are crucial in these products. At present, three types of filter materials are adopted, namely porous membrane, non-woven fiber filter material and nano-fiber filter material. The core performances of filter media are filtration effect and air resistance, but these two performances are mutually restrictive. Porous membrane filter material refers to many small pores on the membrane matrix, such as ePTFE membrane.<sup>9–11</sup> This kind of material has low air flux due to its low porosity, and generally has a very high filtration effect, but the air resistance of which is very large. Non-woven fiber filter material is widely used at present, such as PP melt-blown filter. This kind of material has high porosity and high air flux, but low filtration efficiency.<sup>12,13</sup> In order to achieve high efficiency and low resistance, it is necessary to improve the filtration efficiency with help of static electricity technology.<sup>14–17</sup> However, due to the easily dissipated charge, the filtration efficiency of this filters decrease rapidly in actual use. Nano-fiber filter material is a new kind of filter material with the development of nanotechnology in recent years. Because such materials have small fiber diameters, they can produce nano-scale pores with high specific surface area and high van der Waals forces.<sup>18–28</sup> Chong *et al.* found that the polar chemical groups on PAN nanofibers have a great combination with PM2.5.<sup>18</sup> Carbon nanotube filter material developed by Li *et al.* showed good filtration performance.<sup>19</sup> Many techniques were used to make nanofiber filter materials. Such as electrospinning, melt spinning, CVD, and the like. However, each technology has its limitations. Electrospinning is widely considered as the most promising industrialization manufacturing technology of nanofiber, whose advantages have

<sup>a</sup>State Key Laboratory of New Ceramics and Fine Processing, School of Materials Science and Engineering, Tsinghua University, Beijing 100084, China. E-mail: [huiwu@mail.tsinghua.edu.cn](mailto:huiwu@mail.tsinghua.edu.cn)

<sup>b</sup>School of Materials Science and Technology, China University of Geosciences, Beijing 100083, China

† Electronic supplementary information (ESI) available. See DOI: 10.1039/d0ra01656j

‡ These authors contributed equally to this work.



been proved through a large number of studies. By contrast, several problems gradually reveal in industrial road due to the high cost of the technology, low yield, and the conductive requirements of the substrate, which make electrospinning unable to adapt to the overall filter market demand, and greatly limited in application.<sup>28</sup> In the past, our group provide a new strategy, blow spinning, that can quickly and efficiently prepare nanofibers without the need of a high-voltage electric field.<sup>29–32</sup> Our group independently developed a hand-held spinning device that can directly spray nanofibers on screens to effectively intercept PM<sub>2.5</sub>.<sup>29</sup> The small output of handheld spinning equipment is only suitable for home use, and cannot meet large demand for filter. Hand-held spinning device nanofiber screen technology is only suitable for home applications. Industrial continuous production technology based on blow spinning technology is critical for large-scale application of nanofibers in air filtration. However, scale-up of blow spinning of nanofiber air filters to the industrial level has not been demonstrated so far.

The present work has successfully developed continuous production system of a long-width (500 mm) nanofiber membrane, which can continuously produce multi-level PAN nanofiber filter. At the same time, it can be combined with any substrate based on blow spinning. The specificity of the composite has successfully developed a PAN nanofiber filter compound with a meltblown electrostatic filter material, which can achieve an initial PM<sub>2.5</sub> efficiency of 95%, and maintain

a filtration efficiency of 84.3% during the 20 day test period. According to test analysis, we found that it has obvious advantages when intercepting particle blow 100 nm than melt-blown filter.

The biggest value of our work is to successfully realize the continuous production of 500 mm wide nanofiber membrane by blow spinning. The schematic of the setup used in the continuous production is shown in Fig. 1a. Polymer solution was supplied into the spinneret with corresponding speed. The high-speed air was delivered to spinneret by air compressor. The spinneret consisted of an array of concentric nozzles, whose internal diameter is 0.15 mm. Fig. 1b shows the spinneret is running. It can be observed that multiple liquid jet from the tip of needles. As the solvent evaporates, the fibers eventually form. Fig. S1† demonstrate the actual production system. The rotating mesh is use to collect nanofibers. The nanofiber membranes formed on the mesh by suction, which were collected directly into rolls. Based on our previous research result, we choose PAN polymer as the raw material of nanofiber.<sup>29</sup> Fig. 1c shows a 500 mm wide PAN nanofiber membrane that produced by our setup under optimal process parameters, showing very good uniformity and self-support. The thickness of the membrane can be controlled by changing the different web speeds. Fig. S2† shows nanofiber membrane having thicknesses of  $5 \pm 0.7 \mu\text{m}$ ,  $11 \pm 1.1 \mu\text{m}$ ,  $36 \pm 3.4 \mu\text{m}$  and  $110 \pm 5.4 \mu\text{m}$ , respectively. There are not any holes in nanofibers membrane, indicating the manufacturing process is stable and uninterrupted. In addition

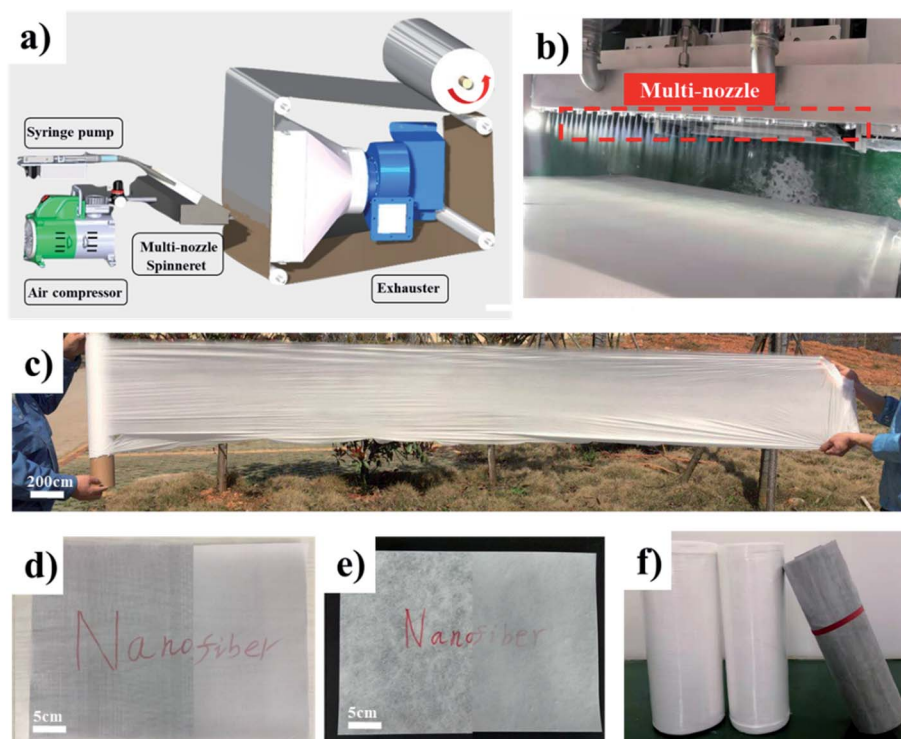


**Fig. 1** (a) Schematic illustration of the continuous production setup for blow spinning. (b) A digital image of multi-nozzles spinneret. (c) A digital image of a roll of nanofiber membranes. (d) Metal mesh before (left) and after (right) nanofibers coating. (e) Spunbond fabrics before (left) and after (right) nanofibers coating. (f) Various rolls of nanofiber composite materials: nanofiber/spunbond fabrics, nanofiber/80 mesh polyester gauze and nanofiber/metal mesh. (from left to right).

to the preparation of self-support nanofiber membranes, our technology was proved to be easily implemented by directly spraying fibers on any substrate. The Fig. 1d shows the fiber spray on metal mesh. We write the word to show the difference between the front and back of the spray fiber. The left picture shows the metal mesh before the fiber spray. The nanofiber words on the right is blurred, showing the nanofiber bond with metal mesh. Nanofibers can also be spray on spunbond fabrics (Fig. 1e), and 80 mesh polyester gauze (Fig. S6†). Various thicknesses of nanofibers can be adopted to deposited on each substrate on needs (Fig. S7†). After being sprayed with nanofibers, the composite filter material can be continuously collected into rolls. Fig. 1f demonstrate various rolls of nanofiber composite materials.

Scan electron microscopy (SEM) was used to observe the morphology of the nanofibers. Fig. 2a shows that the nanofibers have no defects and the fiber surface is very smooth. Under a larger field of view (Fig. 2b), the fibers are interwoven and distributing evenly. The map of fiber diameter (Fig. 2c) indicate that, the average diameter of the fiber is 330 nm, and the fiber diameter is mostly in the range of 250–300 nm, accounting for 30% of the whole. The average pore size of the nanofiber scaffolds is 3.79  $\mu\text{m}$  (Fig. S5†). SEM image (Fig. 2d) shows that the nanofibers are uniformly deposited on the metal mesh without any huge pores. Fig. 2e shows the microscopic morphology of the composite of nanofibers and spunbond fabrics. The surface of spunbond fabrics is rough, which do not influence the uniform distribution of fibers. In fact, the process affects the morphology of the fibers. As Table S1† shows three process parameters. Number 1 is the optimal process we use. However, when the air pressure is increased, a lot of droplets are present on fiber (Fig. S3†). We speculate that the droplets are mainly caused by the turbulence of the air flow increasing with the increase of air pressure. When the flow rate increases, the fiber

bundle was observed in SEM image (Fig. S4†). The generation of fiber bundles is mainly because the solvent is less volatile as the flow rate increases, and the interference between adjacent needles is intensified, which makes uneven distribution of fiber.

There are different requirements for filtration efficiency and pressure drop in various situation of PM<sub>2.5</sub> filtration. On previous studies by our group, PAN nanofiber filter has shown good performance on intercepting particle due to their high polarity. In order to adapt to large-scale production of PAN nanofiber filters, we abandoned the DMF solvent due to huge health risks, and we use green DMSO as the solvent. We choose standard MPPS particle filtration test to evaluate the performance of filter. Fig. 3a shows the test results of different level of filters: PAN60 (filtration efficiency is 63.2%, pressure drop is 18 Pa), PAN80 (filtration efficiency is 80.7%, pressure drop is 38 Pa), PAN90 (filtration efficiency is 92.9%, pressure drop is 58 Pa) PAN99 (filtration efficiency is 99.5%, pressure drop is 123 Pa). In mechanical tensile test, PAN nanofiber filter was broken after being elongated to 13.3%, and the maximum stress was 2.3 MPa. The inset image shows the state in which the fiber membrane is stretched to the maximum elongation. The filtration stability of the filter material is a very important evaluation index of filtration performance but easy to be ignored in actual use. The traditional melt-blow filter material usually adopts to charge in order to achieve high filtration efficiency. However, the dissipation of static electricity will seriously affect the performance of the filter. Fig. 3c shows that the filtration efficiency of the melt-blown electrostatic filter material gradually decreases with the storage time in the environment of 25 °C. The filtration efficiency decreases from the initial 84.3% to 65.4% on the 6th day, which is decreased by 18.9%, and the sample data is highly variable. PAN nanofiber filter material remained stable in filtration efficiency during the

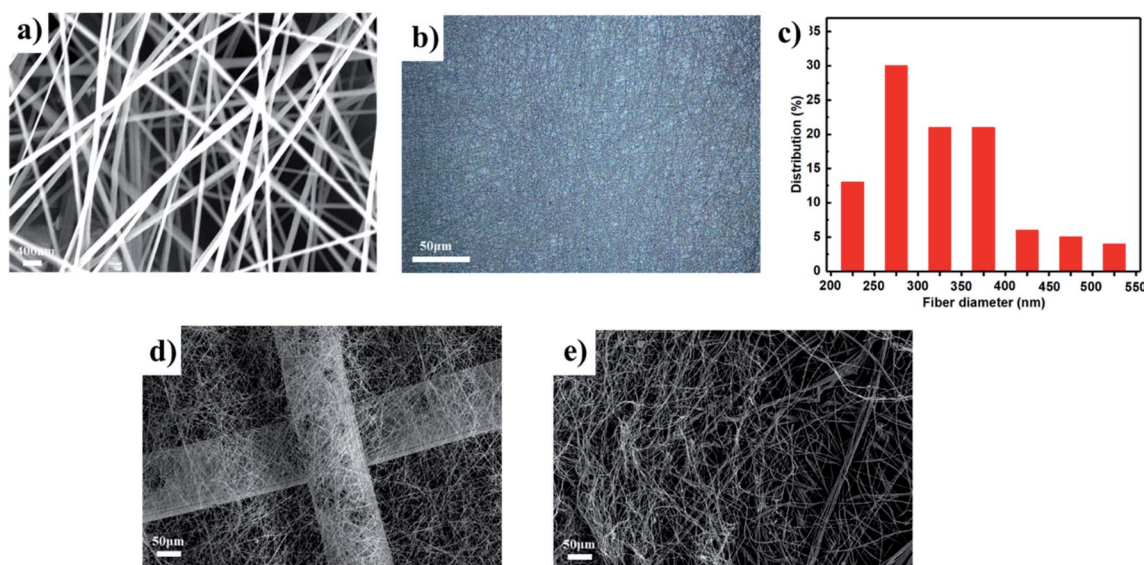


Fig. 2 (a) A SEM image of nanofibers. (b) A optical microscope image of nanofibers. (c) The map of nanofiber diameter. (d) A SEM image of metal mesh with nanofiber coating. (e) A SEM image of spunbond fabrics with nanofiber coating.

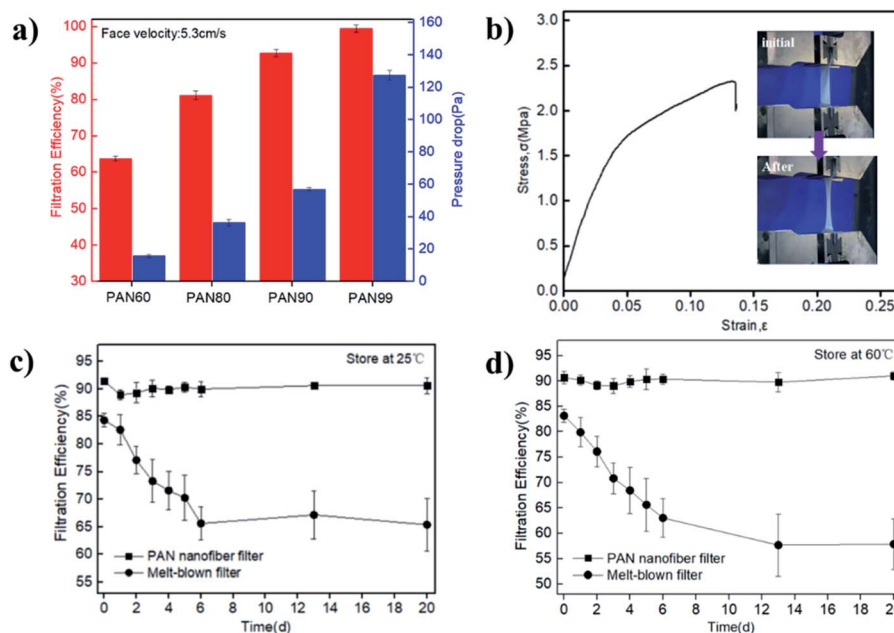


Fig. 3 (a) Filtration efficiency of multi-level PAN nanofiber filters. (b) The curves of tensile strength versus of strain for PAN nanofibers. (c) The long-term performance of filtration efficiency of PAN nanofiber and melt-blown at 25 °C. (d) The long-term performance of filtration efficiency of PAN nanofiber and melt-blown at 60 °C.

20 day storage period. This is mainly because PAN nanofibers interfere with PM<sub>2.5</sub> by relying on PAN polarity attraction and nanofiber physical interception. These two mechanisms are not interfered by environmental factors, resulting in long-term guarantees. Fig. 3d shows that at 60 °C at a higher temperature, the melt-blown filter material continued to decrease over time, and after 20 days the filtration efficiency decreased to 57.9%, a decrease of 25.2%. By contrast, PAN nanofibers remain stable and show better environmental adaptability than melt blown filters.

The melt-blown filter material has lower pressure drop among other kinds of filter, which are usually used in civil field such as mask and air purifier. In fact, when the filter fails in actual situation, users will be exposed to PM<sub>2.5</sub> without knowing it and face health risks. However, melt-blown filter cannot intercept PM<sub>2.5</sub> without charge due to huge size pore of fiber scaffolds. Therefore, we provide a strategy that combine nanofibers with melt-blown filter. PAN nanofibers were sprayed directly on the melt-blown filter by blow spinning. The composite filter can balance stability and low pressure drop. Fig. 4a shows that the initial filtration efficiency of the melt-blown filter material is 83.42%, the initial pressure drop is 21.7 Pa. After PAN nanofibers coating, it was found that the filtration efficiency of the composite filter reached 95.54%, and the pressure drop increased slightly to 29.1 Pa. For testing the efficiency of full-size particle scanning analysis, the PM particles used neutralized monodisperse solid NaCl nanoparticles, which have a diameter from 30 to 600 nm. As shown in Fig. 4b, it is found that the filtration efficiency of the particulate matter under the all the NaCl particle (30–600 nm) is improved. In particular, there is huge improvement on the filtration

efficiency of composite filter for particles below 100 nm. The combination of nanofibers and melt-blown filter, which is also the key to actual use has been evaluated. After adding average 47 g weight, nanofiber finally fall off with melt-blown, an average bond stress of 80.3 N m<sup>-2</sup> (Fig. 4c). From the SEM image of the cross section, PAN nanofiber layer was tightly packed on the melt-blown filter material. It is presumed that the solvent did not completely evaporate after the fiber fell on the substrate. After the solvent was finally evaporated, the nanofibers could effectively adhere to the surface of substrate. As shown in Fig. 4d and e, the environmental resistance of the composite filter is as expected to increase. When testing at 25 °C, the initial efficiency is 94.25%. After 20 days, the final efficiency is 85.03%. There is only a 9.2% decrease in filtration efficiency compared to the initial efficiency. When testing at 60 °C, the initial efficiency is 95.13% and the final efficiency is 79.49% after 20 days. These results indicate that composite filters have more stable filtration performance.

In summary, we successfully realized the continuous production of 500 mm wide nanofiber membrane by blow spinning. This technology can continuous fabrication nanofiber coating on each substrate. Base on this technology, we fabricated multi-level PAN nanofiber filter, namely, PAN60 (filtration efficiency: 63.2%, pressure drop: 18 Pa), PAN80 (filtration efficiency: 80.7%, pressure drop 38 Pa), PAN90 (filtration efficiency: 92.9%, pressure drop: 58 Pa) PAN99 (filtration efficiency: 99.5%, pressure drop: 123 Pa), which have good stability of filtration performance in different situation. In order to improve the stability performance of melt-blown filter, we provide a strategy that combine nanofibers with melt-blown filter. PAN nanofibers were sprayed directly on the melt-blown filter by blow spinning.

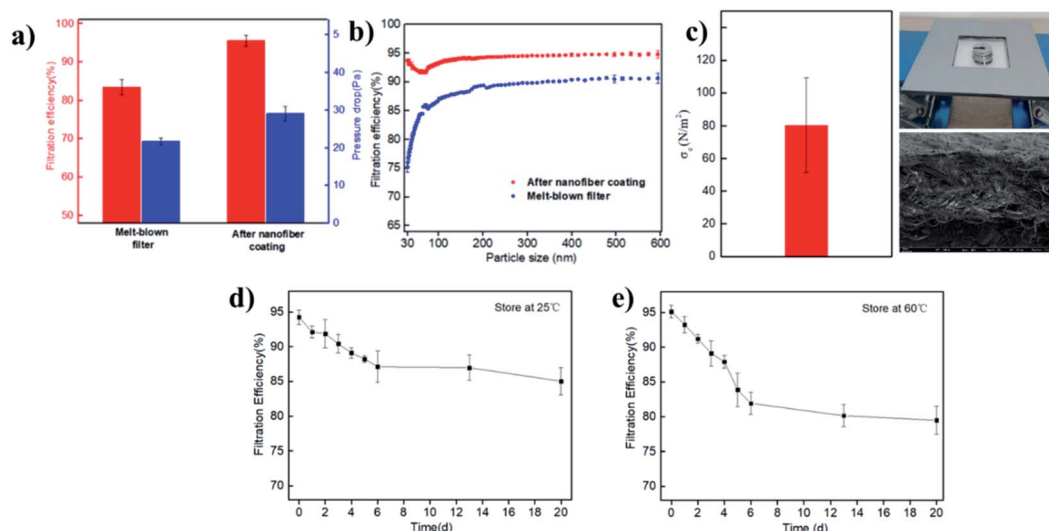


Fig. 4 (a) Filtration efficiency of melt-blown filter before and after nanofibers coating. (b) The filtration efficiency distribution for NaCl particles with different sizes (30–600 nm). (c) The bond stress between nanofiber and melt-blown filter. Inset image: (upper right) the digital image of experimental process; (bottom right) a SEM image of nanofiber/melt-blown surface. (d) The long-term performance of filtration efficiency of composite filter at 25 °C. (e) The long-term performance of filtration efficiency of composite filter at 60 °C.

The composite filter have more stable filtration performance and higher efficiency when intercepting particle blow 100 nm than melt-blown filter. We believe that the continuous production technology of nanofiber by blow spinning offers a new option to protect our environment and personal health more effectively.

## Experimental section

### Solution preparation

For mass production experiments precursor solution was prepared according to a typical process as follows. PAN ( $M_w = 15w$ , Dow) was first dry at 60 °C for 2 h. To obtain a homogenous solution, a 12 wt% polyacrylonitrile (PAN) polymer solution in dimethyl sulfoxide (DMSO, Toray) was stirred under 80 °C for 6 h.

### Setups and experimental procedures

The experimental multi-nozzle setup which are designed and manufactured by our group is depicted in Fig. S1.† Polymer solution is delivered from a syringe pump at rate 130 mL h<sup>-1</sup> to a reservoir attached to the nozzle. Air is supplied through the airway at the pressure of 40–60 kPa. (the gas jet has velocity in 100–120 m s<sup>-1</sup> range). The air is heated at 50 °C. Nanofibers can be deposited onto mesh to directly produce nanofiber membrane by suction. Different level of nanofiber filters can be obtained by adjusting the speed of the mesh (40–250 m h<sup>-1</sup>). When different substrates are put in mesh, nanofibers can deposit on it. PAN nanofibers/melt-blown composite filter was roll-to-roll produced through nanofiber coating on melt-blown filters.

### Characterization

A field-emission scanning electron microscope (let-1530, Zeiss) was adopted to observe the microstructure of the samples. The

diameter of fibers was obtained by measuring the diameter of 200 fibers. The filtration efficiency of filter was evaluated by Automated filter testers (TSI8130A). The MPPS filtration testing, the PM sources were generated from NaCl aerosol particles which were produced by atomized aerosol generator (TSI-3076), and the particle size distribution and concentration of NaCl aerosol were measured by scanning mobility particle sizer (TSI-3936). The procedure of binding force test was shown in Fig. S8.† In order to minimize the test errors in filtration test, 5 samples was used to test. Tensile tests were performed using a Zwick universal testing machine, Zwick Roell Z005.

## Conflicts of interest

There are no conflicts to declare.

## Acknowledgements

This work was supported by the Basic Science Center Program of the National Natural Science Foundation of China (NSFC) under Grant No. 51788104 and NSFC projects under Grant No. 51661135025, National Basic Research of China under Grant No. 2015CB932500. The mass production set-up was designed and manufactured by Shenzhen WeDo New Materials Co., Ltd.

## References

- 1 A. Nel, Air pollution-related illness: effects of particles, *Science*, 2015, **308**, 804–806.
- 2 R. M. Harrison and J. X. Jin, Particulate matter in the atmosphere: which particle properties are important for its effects on health, *Sci. Total Environ.*, 2000, **249**, 85–101.

- 3 C. A. Pope and D. W. Dockery, Health effects of fine particulate air pollution: lines that connect, *J. Air Waste Manage. Assoc.*, 2006, **56**, 709–742.
- 4 R. Zhang, Chemical characterization and source apportionment of PM 2.5 in Beijing: seasonal perspective, *Atmos. Chem. Phys.*, 2013, **13**, 7053–7074.
- 5 H. Wang, Y. H. Zhuang and W. Ying, Long-term monitoring and source apportionment of PM 2.5/PM 10 in Beijing, China, *J. Environ. Sci.*, 2008, **20**, 1323–1327.
- 6 R. D. Brook, Particulate matter air pollution and cardiovascular disease an update to the scientific statement from the American Heart Association, *Circulation*, 2010, **121**, 2331–2378.
- 7 K. L. Timonen, Effects of ultrafine and fine particulate and gaseous air pollution on cardiac autonomic control in subjects with coronary artery disease: the ULTRA study, *J. Exposure Sci. Environ. Epidemiol.*, 2006, **16**, 332–341.
- 8 S. W. Wu, Association of cardiopulmonary health effects with source appointed ambient fine particulate in Beijing, China: a combined analysis from the Healthy Volunteer Natural Relocation (HVNR) study, *Environ. Sci. Technol.*, 2014, **48**, 3438–3448.
- 9 B. H. Park, S. B. Kim and Y. M. Jo, Filtration characteristics of fine particulate matters in a PTFE/glass composite bag filter, *Aerosol Air Qual. Res.*, 2012, **12**, 1030–1036.
- 10 S. Feng, D. Li and Z. Low, ALD-seeded hydrothermally-grown Ag/ZnO nanorod PTFE membrane as efficient indoor air filter, *J. Membr. Sci.*, 2017, **531**, 86–93.
- 11 Y. Bai, C. B. Han and C. He, Washable multilayer triboelectric air filter for efficient particulate matter PM 2.5 removal, *Adv. Funct. Mater.*, 2018, **28**, 1706680.
- 12 X. Du, J. Wei, W. Liu, X. Zhou and D. Dai, Polypropylene nonwoven surface modified through introducing porous microspheres: preparation, characterization and adsorption, *Appl. Surf. Sci.*, 2016, **360**, 525–533.
- 13 M. A. Hassan, B. Y. Yeom and A. Wilkie, Fabrication of nanofiber meltblown membranes and their filtration properties, *J. Membr. Sci.*, 2013, **427**, 336–344.
- 14 M. Nifuku, Y. Zhou and A. Kisiel, Charging characteristics for electret filter materials, *J. Electrostat.*, 2001, **51**, 200–205.
- 15 H. Xiao, Y. Song and G. Chen, Correlation between charge decay and solvent effect for melt-blown polypropylene electret filter fabrics, *J. Electrostat.*, 2014, **72**, 311–314.
- 16 J. Van Turnhout, J. W. C. Adamse and W. J. Hoeneveld, Electret filters for high-efficiency air cleaning, *J. Electrostat.*, 1980, **8**, 369–379.
- 17 Z. Wang and Z. Pan, Preparation of hierarchical structured nano-sized/porous poly(lactic acid) composite fibrous membranes for air filtration, *Appl. Surf. Sci.*, 2015, **356**, 1168–1179.
- 18 C. Liu, P. C. Hsu and H. W. Lee, Transparent air filter for high-efficiency PM 2.5 capture, *Nat. Commun.*, 2015, **6**, 6205.
- 19 P. Li, C. Wang and Y. Zhang, Air filtration in the free molecular flow regime: a review of high-efficiency particulate air filters based on carbon nanotubes, *Small*, 2014, **10**, 4543–4561.
- 20 J. Xu, C. Liu and P. C. Hsu, Roll-to-roll transfer of electrospun nanofiber film for high-efficiency transparent air filter, *Nano Lett.*, 2016, **16**, 1270–1275.
- 21 L. Wang, Y. Kang, C. Y. Xing, K. Guo, X. Q. Zhang and L. S. Ding,  $\beta$ -Cyclodextrin based air filter for high-efficiency filtration of pollution sources, *J. Hazard. Mater.*, 2019, **373**, 197–203.
- 22 S. Jeong, H. Cho and S. Han, High efficiency, transparent, reusable, and active PM 2.5 filters by hierarchical Ag nanowire percolation network, *Nano Lett.*, 2017, **17**, 4339–4346.
- 23 R. Zhang, C. Liu and P. C. Hsu, Nanofiber air filters with high-temperature stability for efficient PM 2.5 removal from the pollution sources, *Nano Lett.*, 2016, **16**, 3642–3649.
- 24 L. Wang, Y. Kang, C. Y. Xing, K. Guo, X. Q. Zhang and L. S. Ding,  $\beta$ -Cyclodextrin based air filter for high-efficiency filtration of pollution sources, *J. Hazard. Mater.*, 2019, **373**, 197–203.
- 25 S. Wang, X. Zhao and X. Yin, Electret polyvinylidene fluoride nanofibers hybridized by polytetrafluoroethylene nanoparticles for high-efficiency air filtration, *ACS Appl. Mater. Interfaces*, 2016, **8**, 23985–23994.
- 26 X. Chen, Y. Xu, M. Liang, Q. Ke, Y. Fang and H. Xu, Honeycomb-like polysulphone/polyurethane nanofiber filter for the removal of organic/inorganic species from air streams, *J. Hazard. Mater.*, 2018, **347**, 325–333.
- 27 R. Zhang, B. Liu and A. Yang, In situ investigation on the nanoscale capture and evolution of aerosols on nanofibers, *Nano Lett.*, 2018, **18**, 1130–1138.
- 28 J. Xue, T. Wu and Y. Dai, Electrospinning and electrospun nanofibers: methods, materials, and applications, *Chem. Rev.*, 2019, **119**, 5298–5415.
- 29 B. Khalid, X. Bai and H. Wei, Direct blow-spinning of nanofibers on a window screen for highly efficient PM 2.5 removal, *Nano Lett.*, 2017, **17**, 1140–1148.
- 30 Y. Huang, X. Bai and M. Zhou, Large-scale spinning of silver nanofibers as flexible and reliable conductors, *Nano Lett.*, 2016, **16**, 5846–5851.
- 31 H. Wang, X. Zhang and N. Wang, Ultralight, scalable, and high-temperature-resilient ceramic nanofiber sponges, *Sci. Adv.*, 2017, **3**, 1603170.
- 32 H. Wang, S. Lin and S. Yang, High-temperature particulate matter filtration with resilient yttria-stabilized ZrO<sub>2</sub> nanofiber sponge, *Small*, 2018, **14**, 1800258.